CAMP^{2}Ex Chemical Influence Flag, Version R0

Version R0 notes: Analysis used version R0 of the Diskin TraceGas CO, CH_4, and O_3 measurements and version R0 of the Diskin DLH H_2O vapor measurements.

General Description

This flag is intended to separate out different chemical regimes observed in the CAMP^{2}Ex dataset, specifically biomass burning versus urban emissions as well as discernible urban sources. These regimes are separated by differences in the populations of enhancement ratios of methane (CH_4) and carbon monoxide (CO). As CO and CH_4 have predominantly slow tropospheric photochemical loss pathways, correlated enhancements between the two are primarily related to the airmass source. Biomass burning has been widely reported in the literature to have low CH_4:CO emission ratios, typically < 10% over a variety of fuels and burning conditions (Nara et al., 2017; Worden et al., 2017). This contrasts with higher CH_4:CO emission ratios reported from fossil fuel combustion, typically closer to 100% (Helfter et al., 2016).

Regime		Description		Flag Value
Background		Air with low enough concentration enhancements that chemical influence could not be determined		0
Clark		Air influenced by local conditions during takeoff and landing		1
Mystery High Ozone		Possibly stratospherically influenced air, but with conflictingly high methane, source unclear		2
Biomass Burning		Observed lower enhancement ratios indicating biomass burning influence		3
Urban/Biomass Burning Mixing		Observed intermediate enhancement ratios indicating mixing between urban-influenced air and biomass burning-influenced air		4
Urban	Uncorrelated	Observed higher enhancement ratios indicating biomass burning influence	No additional discernable source signatures	5
	High CH_4		Additional signatures of stronger CH_4 contribution sources	6
	Low CH_4		Additional signatures of weaker CH_4 contribution sources	7

A combination of two different approaches toward calculating $\Delta CH_4/\Delta CO$ enhancement ratios were used to isolate the biomass burning and urban regimes: one using a single campaign background to determine enhancement ratios and a second using dynamic linear fitting on a rolling time window throughout each flight to find correlated enhancement ratios.

Single Background Method

A single concentration each for CO and CH_4, 65 ppb and 1.85 ppm respectively, were chosen as the background for the full dataset. These were chosen by fitting various segments of the urban and biomass burning lobes of the CH_4 vs CO distribution to determine what a consensus background would be. However, much of the data at small CH_4 and/or CO enhancements above these background levels were

still not separable into urban and biomass burning regimes due to the variability in the true background concentration of each species. Thus, it was necessary to find the minimum ΔCH_4 and ΔCO enhancement above background at which the two regimes begin to be separable but also as low as possible to maximize the data capable of being assigned to each regime. To accomplish this, the frequency distribution of $\Delta CH_4/\Delta CO$ enhancement ratios were examined at various ΔCH_4 and ΔCO enhancement levels above background concentrations (Fig. 1). In these plots, the high data frequency peaks of both the biomass burning regime (at low $\Delta CH_4/\Delta CO$ enhancement ratios) and the urban regime (at high $\Delta CH_4/\Delta CO$ enhancement ratios) are clearly noted. As the cutoff enhancement concentrations increase, a minimum in the frequency distribution emerges between around 35-70%. The optimum cutoff concentration enhancements at which this minimum emerges were found to be 40 ppb for ΔCH_4 and 55 ppb for ΔCO.

Flag categories were then assigned by enhancement ratio and intensity of enhancement with respect to these cutoff concentrations, the results from which are shown in Fig. 3:

Regime	Enhancement Cutoff	Enhancement Ratio Cutoff
Background	Δ CO < 55 ppb & ΔCH_4 < 40 ppb	-
Biomass Burning	ΔCO > 55 ppb	$\Delta CH_4/\Delta CO$ < 35%
Urban/Biomass Burning Mixing	ΔCO > 55 ppb | ΔCH_4 > 40 ppb	$\Delta CH_4/\Delta CO$ > 35% & $\Delta CH_4/\Delta CO$ < 70%
Urban	ΔCH_4 > 40 ppb	$\Delta CH_4/\Delta CO$ > 70%

Ten ppb of hysteresis was added to each of these cutoffs to minimize fast flag switching at interfaces (Fig. 2). To trigger the flag, the concentration of one of the species had to exceed the cutoff + 10 ppb. The flag would remain triggered until the concentration once again fell below the cutoff.

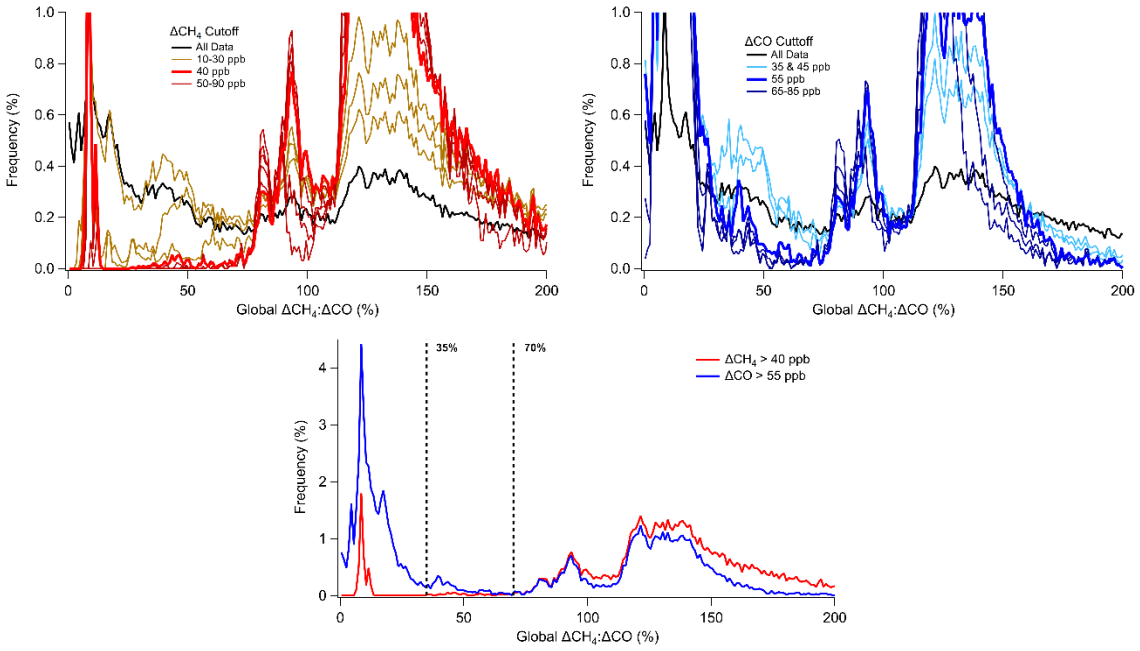

Figure 1: Sensitivity test of $\Delta CH_4/\Delta CO$ emission ratio distributions to concentration cutoffs in CH_4 (upper-left) and CO (upper-right). Bottom plot shows the optimum cutoff for each species along with the minimum range in the distribution chosen to separate the regimes.

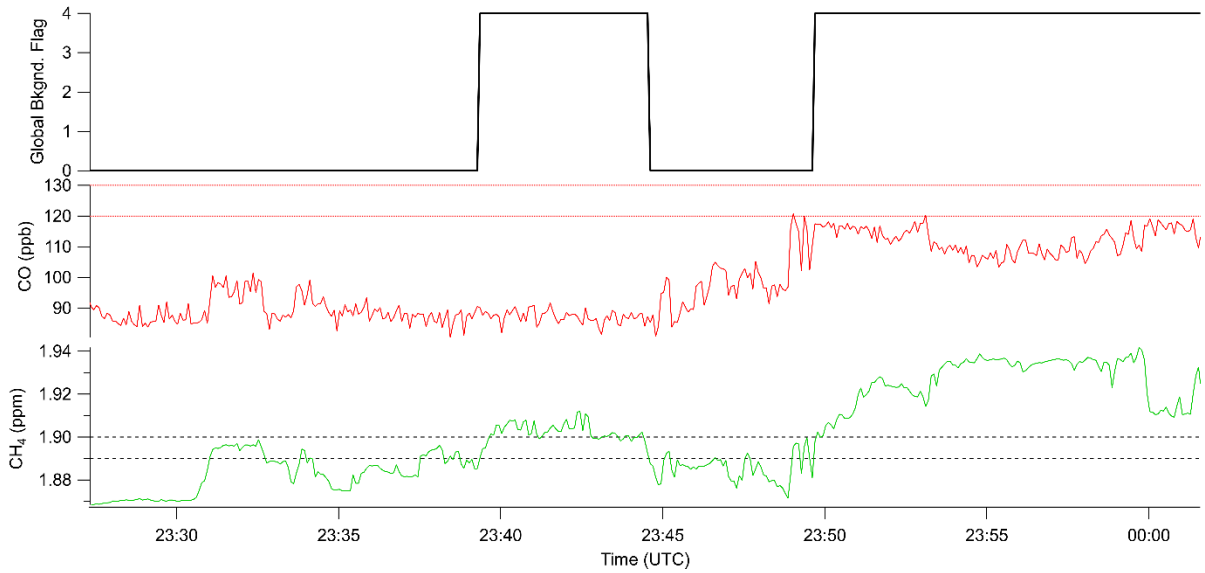

Figure 2: Example of hysteresis in identifying urban influence.

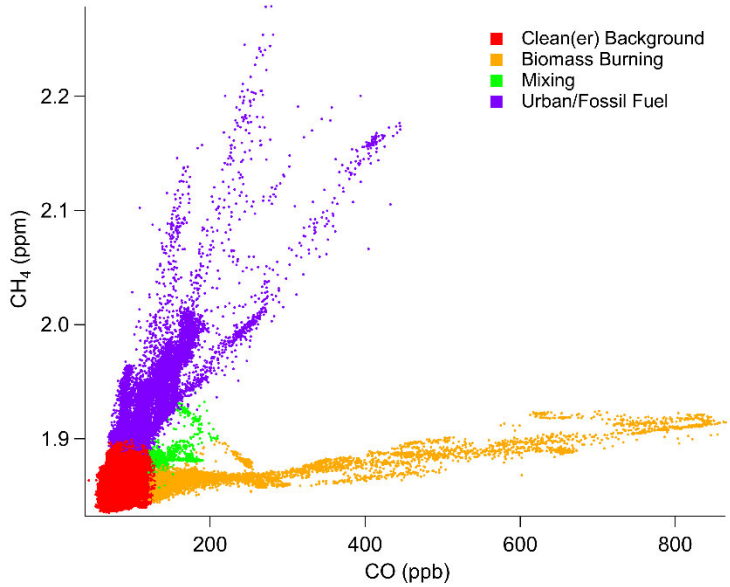

Figure 3: Results of Single Background analysis.

Rolling Slope Approach:

As the single background technique is limited due to the coarse assumption of a constant chemical background over the entirety of the campaign, a different approach was used to extract more fine detailed information from the dataset. With this approach, the linear fits of CH_4 vs CO were calculated using weighted orthogonal distance regression (ODRPACK95 - IGOR Pro v7; Wu & Yu, 2018) for 2 min rolling windows through each flight, similar to the technique used by Halliday et al. (2019) for $\Delta CO/\Delta CO_2$ enhancement ratios. Fits with lower goodness of fit ($r^2 < 0.5$) were filtered as uncorrelated. Slopes

from the remaining fits represented a $\Delta CH_4/\Delta CO$ enhancement ratio product that is independent of changes in background concentration. In the frequency distribution of the $\Delta CH_4/\Delta CO$ slopes, four regimes were apparent (Fig. 4): a negative-sloped regime that corresponded to mixing lines between urban-influenced and biomass burning-influenced air; a biomass burning regime peaking in the small (<10%) $\Delta CH_4/\Delta CO$ slope region; an intermediate regime peaking around 60-80% $\Delta CH_4/\Delta CO$; and a high slope regime that was asymptotic toward high $\Delta CH_4/\Delta CO$. Numerically, these were defined as:

Regime	$\Delta CH_4/\Delta CO$ Limits
Urban/Biomass Burning Mixing	$\Delta CH_4/\Delta CO < 0\%$
Biomass Burning	$\Delta CH_4/\Delta CO > 0\%$ & $\Delta CH_4/\Delta CO < 40\%$
Urban Low CH_4 Regime	$\Delta CH_4/\Delta CO > 40\%$ & $\Delta CH_4/\Delta CO < 100\%$
Urban High CH_4 Regime	$\Delta CH_4/\Delta CO > 100\%$

The resulting flag was manually filtered to merge clearly temporally contiguous airmasses that may only have had correlation over a portion of the sampling region. Fig. 5 shows the resulting regimes from this analysis.

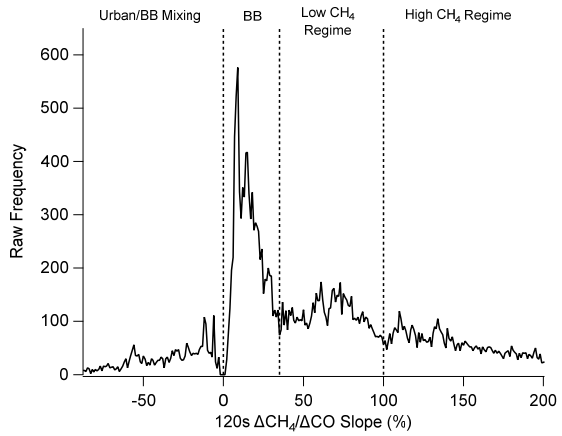

Figure 4: Frequency Distribution of Rolling Slope $\Delta CH_4/\Delta CO$ Enhancement Ratios

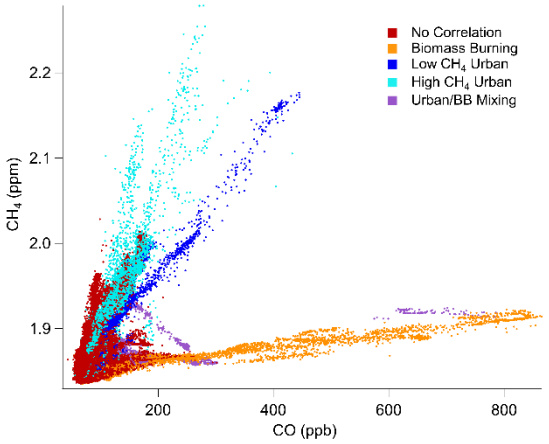

Figure 5: Summary of Rolling Slope Enhancement Ratio Regimes

Clark-Influenced Air

Data influenced by strong local sources during takeoff and landing at Clark International Airport were flagged from takeoff until the first sharp gradient in trace gas concentration/humidity or, if no gradient was discernable, until 1 km AGL. Similarly, Clark influence prior to landing was flagged as either the last sharp trace gas concentration/humidity gradient or 1 km AGL through the end of the flight.

Mystery High Ozone

This consists of data with a strong anticorrelation between ozone and water vapor data (Fig. 6b) at low water mixing ratios (< 8000 ppm_v). This is typically a signature of stratospheric mixing, which would normally result in anti-correlations between ozone and both CH_4 and CO (Figs. 6c&d, respectively). In contrast, these ozone observations are uncorrelated with CO and appear positively correlated with CH_4, suggesting a different chemical source or dynamic process. These data are being actively studied, and an update to the flag will be forthcoming with any new findings.

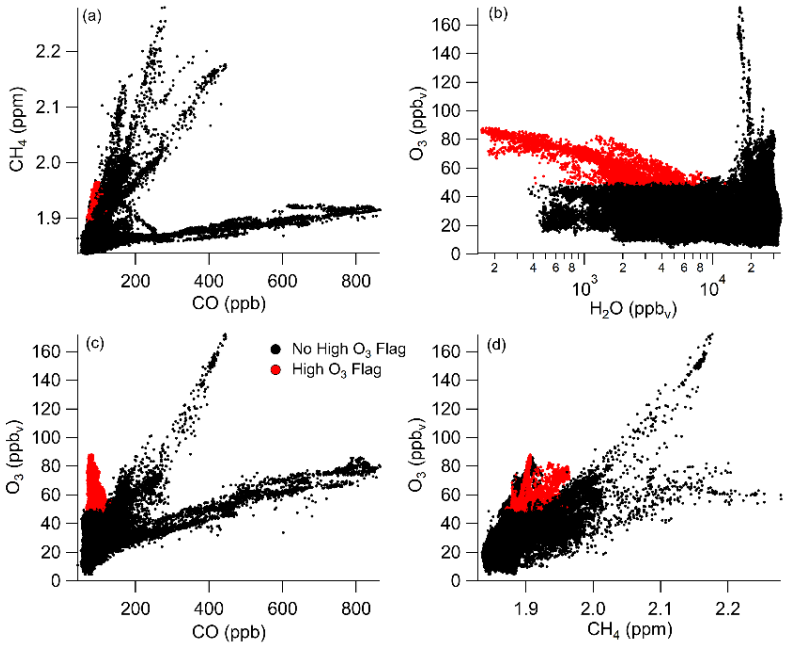

Figure 6: Highlighted data from the Mystery High Ozone flag.

Final Combined Product:

The final combined flag product combined the single background flag and rolling slope flags as follows:

Final Product Regime	Final Product Value	Single Background Regime	Rolling Slope Regime
Background	0	Background	-
Clark (TO/LND)	1	-	-
Mystery High Ozone	2	-	-
Biomass Burning	3	Biomass Burning	-
Urban/Biomass Burning Mixing	4	Urban/Biomass Burning Mixing (from either)	
Urban Uncorrelated	5	Urban	Urban w/No Correlation
Urban Low CH_4	6	Urban	Urban Low CH_4
Urban High CH_4	7	Urban	Urban High CH_4

The final flag background and biomass burning regimes were taken as the same as from the single background method. The urban regime from the single background method was split into three separate regimes based on the correlated slope (or lack thereof) from the rolling slope method. Finally, any non-background data in either of the urban/biomass burning mixing categories were placed in the final urban/biomass burning mixing regime. Figure 7 shows the final regime apportionments with respect to CH_4 and CO.

One Last Caveat: Urban Uncorrelated Data

As a result of this combined product from the differing background methods, one notable flag category is the Urban Uncorrellated data. In this category, the single background method returned an urban signature, but no significant short-term correlation was observed through the rolling slope method. As the bulk slope of that method is consistent with urban enhancement ratios, it seemed reasonable to continue to classify this air as "urban", albeit in a different category to distinguish the greater uncertainty in the assignment.

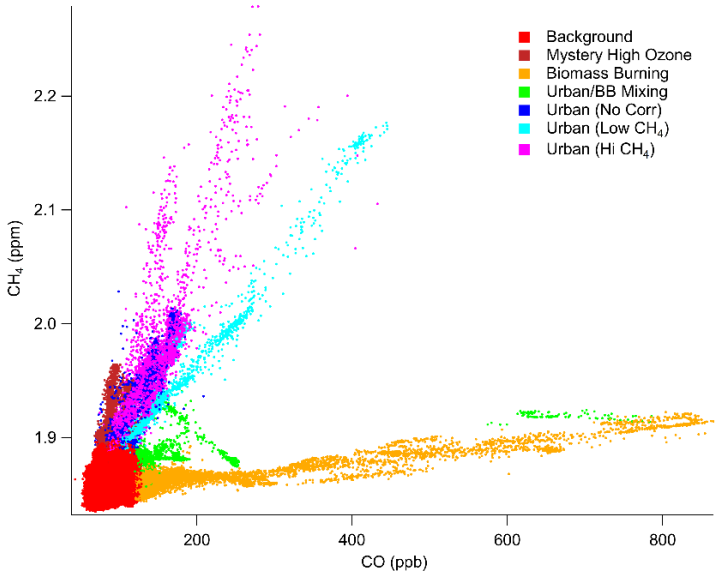

Figure 7: Final flag values (without Clark data)

References:

Halliday, H. S., DiGangi, J. P., Choi, Y., Diskin, G. S., Pusede, S. E., Rana, M., Nowak, J. B., Knote, C., Ren, X., He, H., Dickerson, R. R., & Li, Z. (2019). Using Short-Term CO/CO_2 Ratios to Assess Air Mass Differences Over the Korean Peninsula During KORUS-AQ. *Journal of Geophysical Research: Atmospheres*, *124*(20), 10951–10972. https://doi.org/10.1029/2018JD029697

Helfter, C., Tremper, A. H., Halios, C. H., Kotthaus, S., Bjorkegren, A., Grimmond, C. S. B., Barlow, J. F., & Nemitz, E. (2016). Spatial and temporal variability of urban fluxes of methane, carbon monoxide and carbon dioxide above London, UK. *Atmospheric Chemistry and Physics*, *16*(16), 10543–10557. https://doi.org/10.5194/acp-16-10543-2016

Nara, H., Tanimoto, H., Tohjima, Y., Mukai, H., Nojiri, Y., & Machida, T. (2017). Emission factors of CO2, CO and CH4 from Sumatran peatland fires in 2013 based on shipboard measurements. *Tellus B: Chemical and Physical Meteorology*, *69*(1), 1399047. https://doi.org/10.1080/16000889.2017.1399047

Worden, J. R., Bloom, A. A., Pandey, S., Jiang, Z., Worden, H. M., Walker, T. W., Houweling, S., & Röckmann, T. (2017). Reduced biomass burning emissions reconcile conflicting estimates of the post-2006 atmospheric methane budget. *Nature Communications*, *8*(1), 2227. https://doi.org/10.1038/s41467-017-02246-0

Wu, C., & Yu, J. Z. (2018). Evaluation of linear regression techniques for atmospheric applications: The importance of appropriate weighting. *Atmospheric Measurement Techniques*, *11*(2), 1233–1250. https://doi.org/10.5194/amt-11-1233-2018